

# Electronic Structure and Unimolecular Reactions of Cyclopropenone Carbonyl Oxide. A Theoretical Study<sup>†</sup>

Josep Maria Anglada\*<sup>‡</sup> and Josep Maria Bofill<sup>§</sup>

Centre d'Investigació i Desenvolupament del CSIC, Jordi Girona 18,  
E-08034 Barcelona, Catalunya, Spain, and Departament de Química Orgànica, Universitat de Barcelona,  
Martí i Franquès 1, E-08028 Barcelona, Catalunya, Spain

Received November 1, 1996 (Revised Manuscript Received February 25, 1997<sup>®</sup>)

A theoretical investigation on the lowest singlet and triplet potential energy surfaces of cyclopropenone carbonyl oxide **1** is presented. The calculated equilibrium geometry and dipole moment suggest that **1** possesses a strong zwitterionic character. The energy barrier for the isomerization of **1** to the cyclic isomer dioxirane **2** is computed to be 9.4 kcal/mol. The singlet state of **1** dissociates into cyclopropenone and excited singlet oxygen atom (<sup>1</sup>D), while the triplet state of **1** dissociates yielding oxygen atom in its ground state (<sup>3</sup>P). The dissociation process is endothermic for the singlet state but highly exothermic for the triplet.

## Introduction

The study of carbonyl oxides has become a growing area of interest in the last few years due to their role in several areas of chemistry. The involvement of carbonyl oxides has been discussed in many oxidation reactions (e.g., ozonolysis, Baeyer–Villiger reaction),<sup>1–3</sup> enzymatic processes,<sup>4</sup> the chemistry of urban air pollution,<sup>5</sup> and also in chemical mimics of biological oxygen transfer systems.<sup>6</sup> The importance of carbonyl oxides is reflected in the number of reviews published in the last few years.<sup>2,3b,7</sup>

The electronic nature and geometrical structure of carbonyl oxides have originated a certain amount of controversy that has mainly been addressed to the different degree of zwitterionic or biradical character of these species. Carbonyl oxides were first postulated as intermediates in the ozonolysis of olefins by Criegee<sup>1,8</sup> and originally were formulated as zwitterions. Several substituted carbonyl oxides and their isomeric dioxiranes have been detected and characterized by spectroscopic methods,<sup>9–13</sup> and quite a large number of theoretical studies on carbonyl oxides has been reported in the literature.<sup>14–28</sup> The main theoretical effort in elucidating

their electronic structure has been focused on the prototype formaldehyde carbonyl oxide (H<sub>2</sub>CO<sub>2</sub>)<sup>15,16,19,20,25–27</sup> which has not been observed experimentally yet. Earlier ab-initio calculations on H<sub>2</sub>CO<sub>2</sub> suggested a strong biradical character,<sup>15,16</sup> but more recent ab-initio studies, employing higher levels of theory, indicate an electronic structure with some zwitterionic character.<sup>20i,25b,27</sup> On the other hand, the main theoretical studies on substituted carbonyl oxides have been carried out using semiempirical methods. Ab initio calculations have been reported only for monofluorocarbonyl oxide,<sup>20f</sup> difluorocarbonyl oxide,<sup>28</sup> and acetaldehyde carbonyl oxide.<sup>20a,27</sup>

(10) (a) Sander, W. *Angew. Chem., Int. Ed. Engl.* **1986**, *25*, 255. (b) Sander, W. *Spectrochim. Acta* **1987**, *43A*, 637. (c) Sander, W. *J. Org. Chem.* **1988**, *53*, 125. (d) Sander, W. *J. Org. Chem.* **1988**, *53*, 2091. (e) Sander, W. *J. Org. Chem.* **1989**, *54*, 333.

(11) Ganzer, G. A.; Sheridan, R. S.; Liu, M. T. H. *J. Am. Chem. Soc.* **1986**, *108*, 1517.

(12) (a) Werstiuk, N. H.; Casal, H. L.; Scaiano, J. C. *Can. J. Chem.* **1984**, *62*, 2391. (b) Casal, H. L.; Tanner, M.; Werstiuk, N. H.; Scaiano, J. C. *J. Am. Chem. Soc.* **1985**, *107*, 4616. (c) Barcus, R. L.; Hadel, L. M.; Johnston, L. J.; Platz, M. S.; Savino, T. G.; Scaiano, J. C. *J. Am. Chem. Soc.* **1986**, *108*, 3928. (d) Scaiano, J. C.; McGimpsey, W. G.; Casal, H. L. *J. Org. Chem.* **1989**, *54*, 1612.

(13) (a) Fujiwara, Y.; Tanimoto, Y.; Itoh, M.; Hirai, K.; Tomioka, H. *J. Am. Chem. Soc.* **1987**, *109*, 1942. (b) Murata, S.; Tomioka, H.; Kawase, T.; Oda, M. *J. Org. Chem.* **1990**, *55*, 4502.

(14) Ha, T.-K.; Kühne, H.; Vaccani, S.; Günthard, H. H. *Chem. Phys. Lett.* **1974**, *24*, 172.

(15) (a) Wadt, W. R.; Goddard, W. A., III *J. Am. Chem. Soc.* **1975**, *97*, 3004. (b) Harding, L. B.; Goddard, W. A., III *J. Am. Chem. Soc.* **1978**, *100*, 7180.

(16) (a) Hiberty, P. *J. Am. Chem. Soc.* **1976**, *98*, 6088. (b) Hiberty, P.; Leforestier, C. *J. Am. Chem. Soc.* **1978**, *100*, 2012. (c) Hiberty, P. C.; Devidal, J. P. *Tetrahedron* **1979**, *68*, 4323.

(17) Hull, L. A. *J. Org. Chem.* **1978**, *43*, 2780.

(18) (a) Yamaguchi, K.; Ohta, K.; Yabushita, S.; Fueno, T. J. *J. Chem. Phys.* **1978**, *68*, 4323. (b) Yamaguchi, K.; Yabushita, S.; Fueno, T. J.; Morokuma, K.; Iwata, S. *Chem. Phys. Lett.* **1980**, *71*, 563. (c) Yamaguchi, K. *J. Mol. Struct. (THEOCHEM)* **1983**, *103*, 101.

(19) (a) Karlström, G.; Engström, S.; Jönsson, B. *Chem. Phys. Lett.* **1979**, *67*, 343. (b) Karlström, G.; Roos, B. O. *Chem. Phys. Lett.* **1981**, *79*, 416.

(20) (a) Cremer, D. *J. Am. Chem. Soc.* **1979**, *101*, 7199. (b) Cremer, D. *J. Am. Chem. Soc.* **1981**, *103*, 3619, 3627, 3633. (c) Cremer, D. *Angew. Chem., Int. Ed. Engl.* **1981**, *20*, 888. (d) Cremer, D. In *The Chemistry of Functional Groups, Peroxides*, Patai, S., Ed.; Wiley: New York, 1983; p 1. (e) Gauss, J.; Cremer, D. *Chem. Phys. Lett.* **1987**, *133*, 420. (f) Cremer, D.; Schmidt, T.; Gauss, J.; Radhakrishnan, T. P. *Angew. Chem., Int. Ed. Engl.* **1988**, *27*, 427. (g) Gauss, J.; Cremer, D. *Chem. Phys. Lett.* **1989**, *163*, 549. (h) Cremer, D.; Schmidt, T.; Sander, W.; Bischof, P. *J. Org. Chem.* **1989**, *54*, 2515. (i) Cremer, D.; Gauss, J.; Kraka, E.; Stanton, J. F.; Bartlett, R. J. *Chem. Phys. Lett.* **1993**, *209*, 547.

(21) Kahn, S. D.; Hehre, W. J.; Pople, J. A. *J. Am. Chem. Soc.* **1987**, *109*, 1871.

(22) Rahman, M.; McKee, M.; Shevlin, P. B.; Szytyrbicka, R. *J. Am. Chem. Soc.* **1988**, *110*, 4002.

<sup>†</sup> Dedicated to Professor J. Bertran on the occasion of his 65th birthday.

<sup>‡</sup> Centre d'Investigació i Desenvolupament del CSIC. E-mail: anglado@qteor1.cid.csic.es.

<sup>§</sup> Departament de Química Orgànica, Universitat de Barcelona. E-mail: jmbofill@canigo.qo.ub.es.

<sup>®</sup> Abstract published in *Advance ACS Abstracts*, April 1, 1997.

(1) Criegee, R. *Angew. Chem., Int. Ed. Engl.* **1975**, *14*, 745.

(2) Adam, W.; Curci, R.; Edwards, J. O. *Acc. Chem. Res.* **1989**, *22*, 205.

(3) (a) Murray, R. W.; Ramachandran, V. *Photochem. Photobiol.* **1979**, *30*, 187. (b) Murray, R. W. *Chem. Rev.* **1989**, *89*, 1187.

(4) Dix, T. A.; Benkovic, S. *Acc. Chem. Res.* **1988**, *21*, 101.

(5) (a) Atkinson, R.; Carter, W. P. L. *Chem. Rev.* **1984**, *84*, 437. (b) Atkinson, R.; Lloyd, A. *J. Phys. Chem. Ref. Data* **1984**, *13*, 315.

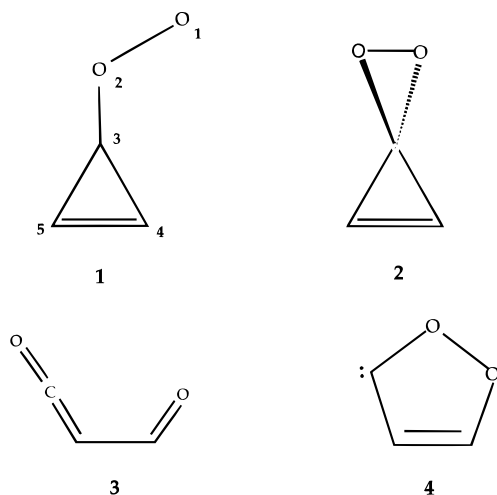
(6) Hamilton, G. A. In *Molecular Mechanisms of Oxygen Activation*; Hayashi, O., Ed.; Academic: New York, 1974, pp 245–283.

(7) (a) Kafafi, R. I.; Martinez, R. I.; Herron, J. T. In *Molecular Structure and Energetics. Unconventional Chemical Bonding*; Liebman, J. F., Greenberg, A., Eds.; VCH Publishers: New York, 1988; Vol. 6, p 283. (b) Murray, R. W. In *Molecular Structure and Energetics. Unconventional Chemical Bonding*; Liebman, J. F., Greenberg, A., Eds.; VCH Publishers: New York, 1988; Vol. 6, p 311. (c) Sander, W. *Angew. Chem., Int. Ed. Engl.* **1990**, *29*, 344. (d) Bunnelle, W. *Chem. Rev.* **1991**, *91*, 335.

(8) Criegee, R.; Wenner, G. *Chem. Ber.* **1949**, *564*, 9.

(9) (a) Bell, G. A.; Dunkin, I. R. *J. Chem. Soc., Chem. Commun.* **1983**, 1213. (b) Dunkin, I. R.; Bell, G. A. *Tetrahedron* **1985**, *41*, 339.

(c) Bell, G. A.; Dunkin, I. R.; Shields, C. J. *Spectrochim. Acta* **1985**, *41A*, 1221. (d) Dunkin, I. R.; Shields, C. J. *J. Chem. Soc., Chem. Commun.* **1986**, 154. (e) Dunkin, I. R.; Bell, G. A.; McCleod, F. G.; McCluskey, A. *Spectrochim. Acta* **1986**, *42A*, 567.



We present here a theoretical investigation on the electronic structure of cyclopropenone carbonyl oxide **1**. This carbonyl oxide is interesting because it is the simplest substituted carbonyl oxide showing a CC double bond conjugated with the COO group. In addition we have also investigated some unimolecular isomerizations of **1**. These include the cyclization of **1** to the cyclopropenedioxirane **2**, the *syn/anti* interconversion of **1**, and the isomerization to produce formylketene **3**. We have also investigated the possibility that the last step could take place through the carbene **4**. Furthermore, we report the most characteristic trends of the potential energy surface (PES) of the lowest triplet state of **1**, as well as the corresponding dissociation energies.

### Computational Details

The basis set used in all geometry optimizations was the split-valence d-polarized 6-31G(d).<sup>29</sup> Molecular geometries of the stationary points located on the aforementioned PESs were optimized by use of multiconfigurational SCF (MCSCF) wave functions of the complete active space (CAS)SCF class<sup>30</sup> employing analytical gradient procedures.<sup>31</sup> The CASs were selected according to the fractional occupation of the natural orbitals (NOs) generated from the first-order density matrix calculated from a MRDCI (multireference single- and double-excitation configuration interaction) wave function,<sup>32</sup> correlating all valence electrons. Thus, for the singlet state of **1** ( $C_s$  molecular symmetry) the fractional occupancies of the NOs indicated that there are ten *active* orbitals. These are six molecular orbitals (MOs) of  $a'$  symmetry, which correspond to the bonding and antibonding orbitals of the  $C_3C_5$ , CO, and OO  $\sigma$  bonds, and four MOs of  $a''$  symmetry. The latter MOs correspond to the bonding and antibonding orbitals of the CC and CO double bonds. Distribution of the corresponding ten *active* electrons, namely, six  $\sigma$  electrons and four  $\pi$  electrons, among these ten *active* orbitals leads to CASSCF(10,10) wave

function formed as a linear combination of 19404 spin-adapted configurations state functions (CSFs) for the singlet state in  $C_1$  symmetry. For the singlet state of **2** ( $C_{2v}$  molecular symmetry) the CASSCF wave function chosen consists in 12 active electrons and 11 active orbitals (the active orbitals are three of  $a_1$ , two of  $a_2$ , two of  $b_1$ , and four of  $b_2$  symmetry, respectively). This space leads to 60984 CSFs in  $C_1$  symmetry. The CASSCF wave function of **3** ( $C_s$  molecular symmetry) consists in 8 active electrons and 7 active orbitals (the active orbitals are three of  $a'$  and four of  $a''$  symmetry) leading to 490 CSFs in  $C_1$  symmetry. Regarding the other stationary points located on the PESs, the active space selection procedure used led to a CASSCF(8,8) wave function formed by linear combination of 1764 CSFs for the singlet and 2352 CSFs for the triplet in  $C_1$  symmetry.

The normal modes and harmonic vibrational frequencies of the equilibrium and transition structures optimized at the CASSCF level of theory were obtained by diagonalization of the mass-weighted Cartesian force constant matrix, calculated numerically by finite differences of analytical gradients.<sup>33a</sup> The dipole moment derivatives that determine the IR intensities were determined by numerically differentiating the dipole moments with respect to the nuclear coordinates and transforming them to normal coordinates.<sup>33b</sup> The zero-point vibrational energies (ZPVEs) were determined from the harmonic vibrational frequencies scaled by 0.8929 (the reciprocal of 1.12).<sup>34</sup> All CASSCF calculations were carried out by using the GAMESS system of programs.<sup>35</sup>

To incorporate the effect of dynamical valence-electron correlation on the relative energy ordering of the calculated stationary points, MRDCI calculations were carried out at the CASSCF optimum geometries using the program package of Buenker and Peyerimhoff,<sup>36</sup> which includes a table CI algorithm and extrapolation techniques. In this MRDCI treatment the reference set consists of all configurations that appear in the final CI expansion with a coefficient of roughly  $c^2 \geq 0.02$ . The CASSCF MOs for the respective states are employed to construct the configurations; all nonvalence MOs are frozen. Configuration selection is undertaken at a threshold of  $T = 6 \mu\text{hartree}$  in a standard manner,<sup>36a</sup> and the resulting secular equation is solved directly. The effect of the remaining configurations of the total MRDCI space on the energy of the system is accounted for by a self-correcting perturbation-type (extrapolation) procedure.<sup>36b,c</sup> Finally, the energy corresponding to the full CI space of the given basis set, designated  $E(\text{MRDCI}+Q)$ , is estimated in analogy to the formula given by Langhoff and Davidson.<sup>37,38</sup> The MRDCI calculations of the stationary points on the  $C_3H_2O_2$  singlet PESs were carried out with the 6-31G(d) basis set. The sizes of the generated MRDCI spaces are of the order of 11 million, while the size of the selected subspaces, namely, the dimensions of the secular equations actually solved, was on the order of 20000–32000.

### Results and Discussion

The most relevant geometrical parameters of the CASSCF-optimized structures of the stationary points

(33) (a) Pulay, P. In *Modern Theoretical Chemistry*; Schaefer, H. F., Ed.; Plenum: New York, 1977; Vol. 4, p 153. (b) Pulay, P.; Fogarasi, G.; Pang, F.; Boggs, J. E. *J. Am. Chem. Soc.* **1979**, *101*, 2550.

(34) Curtiss, L. A.; Raghavachari, K.; Trucks, G. W.; Pople, J. A. *J. Chem. Phys.* **1991**, *94*, 7221.

(35) Schmidt, M. W.; Baldridge, K. K.; Boatz, J. A.; Jensen, J. H.; Koseki, S.; Gordon, M. S.; Nguyen, K. A.; Windus, T. L.; Elbert, S. T. *Gamess. QCPE Bull.* **1990**, *10*, 52.

(36) (a) Buenker, R. J.; Peyerimhoff, S. D. *Theor. Chim. Acta* **1974**, *35*, 33. (b) Buenker, R. J.; Peyerimhoff, S. D. *Theor. Chim. Acta* **1975**, *39*, 217. (c) Buenker, R. J.; Peyerimhoff, S. D.; Butscher, W. *Mol. Phys.* **1978**, *35*, 771. (d) Buenker, R. J.; Peyerimhoff, S. D. In *New Horizons of Quantum Chemistry*; Lowdin, P. O., Pullman, B., Eds.; D. Reidel: Dordrecht, 1983; p 183. (e) Buenker, R. J.; Philips, R. A. *J. Mol. Struct. (THEOCHEM)* **1985**, *123*, 291.

(37) Davidson, E. R. In *New Horizons of Quantum Chemistry*; Lowdin, P. O., Pullman, B., Eds.; D. Reidel: Dordrecht, 1983; p 17. (b) Langhoff, S. R.; Davidson, E. R. *Int. J. Quantum Chem.* **1974**, *8*, 61.

(38) (a) Buenker, R. J.; Peyerimhoff, S. D.; Bruna, P. J. In *Computational Theoretical Organic Chemistry*, NATO ASI; Csizmadia, I. G., Daudel, R., Eds.; D. Reidel: Dordrecht, 1981; p 55. (b) Burton, P. G.; Buenker, R. J.; Bruna, P. J.; Peyerimhoff, S. D. *Chem. Phys. Lett.* **1983**, *95*, 379.

(23) Steinke, T.; Hänsele, E.; Clark, T. *J. Am. Chem. Soc.* **1989**, *111*, 9107.

(24) Yang, C.; You-Liang, W. *J. Mol. Struct. (THEOCHEM)* **1990**, *204*, 285.

(25) (a) Bach, R. D.; Owensby, A. L.; Andrés, J. L.; Schlegel, H. B. *J. Am. Chem. Soc.* **1991**, *113*, 7031. (b) Bach, R. D.; Andrés, J. L.; Owensby, A. L.; Schlegel, H. B.; McDouall, J. J. W. *J. Am. Chem. Soc.* **1992**, *114*, 7207.

(26) Bernhardsson, A.; Lindh, R.; Karlström, G.; Roos, B. O. *Chem. Phys. Lett.* **1996**, *251*, 141.

(27) Anglada, J. M.; Bofill, J. M.; Olivella, S.; Solé, A. *J. Am. Chem. Soc.* **1996**, *118*, 4636.

(28) Rahman, M.; Mckee, M. L.; Shevlin, P. B.; Szyrbicka, R. *J. Am. Chem. Soc.* **1988**, *110*, 4402.

(29) Hariharan, P. C.; Pople, J. A. *Theor. Chim. Acta* **1973**, *28*, 213.

(30) For a review, see: Roos, B. O. *Adv. Chem. Phys.* **1987**, *69*, 399.

(31) (a) Bofill, J. M., *J. Comput. Chem.* **1994**, *15*, 1. (b) Bofill, J. M., Comajuan, M. *J. Comput. Chem.* **1996**, *16*, 1326.

(32) Anglada, J. M.; Bofill, J. M. *Chem. Phys. Lett.* **1995**, *243*, 151.

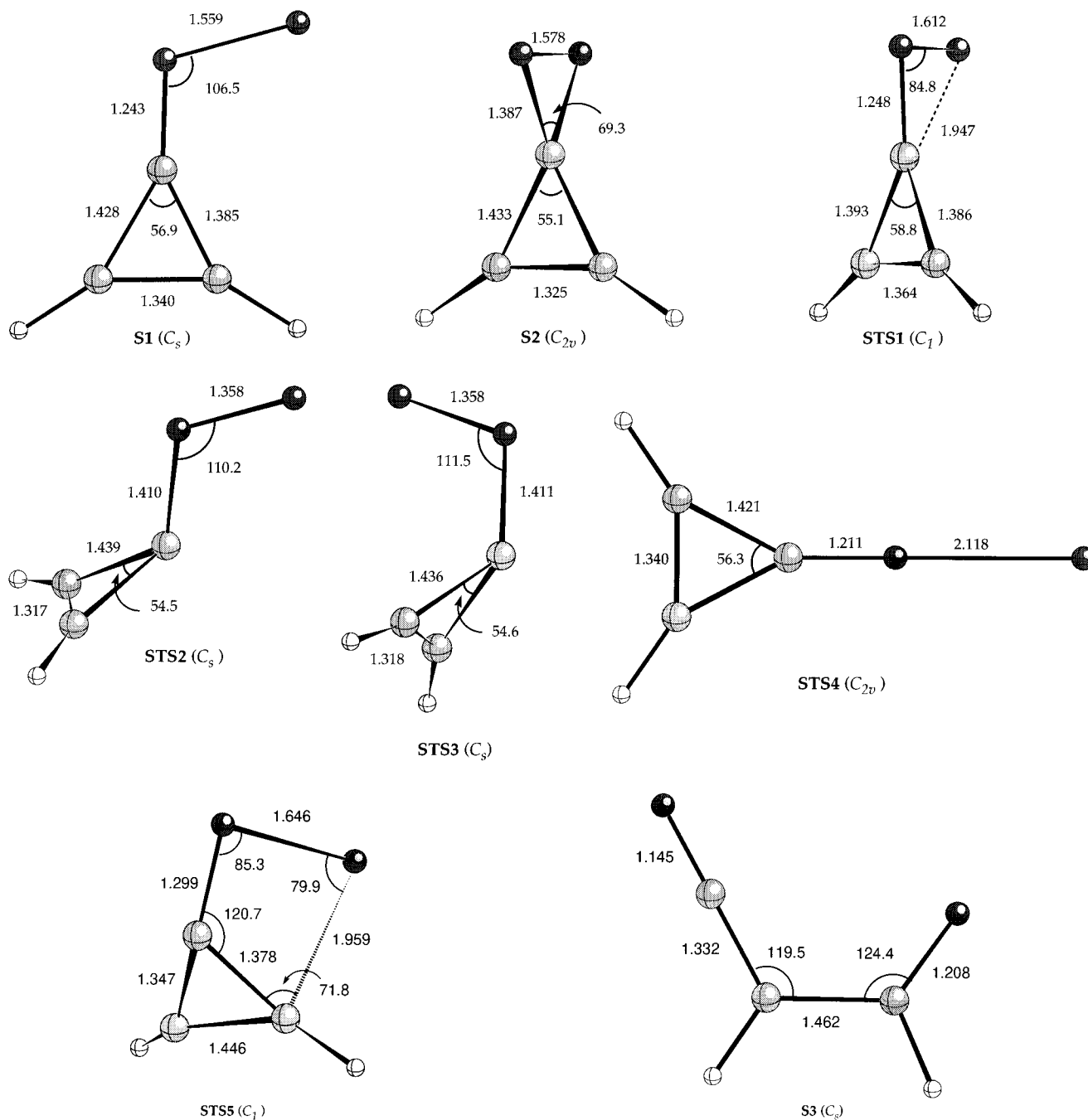


**Figure 1.** Selected geometrical parameters of the CASSCF optimized structures for the stationary points located on the singlet potential energy surface. Distances are given in angstroms and angles in degrees.

located on the singlet and triplet PESs of **1** are given in Figures 1 and 2. These structures are designated by **S** and **T** for the singlet and triplet, respectively. The label of the structures corresponding to transition states is followed by the letters **TS**. Further, the structures are distinguished from each other by appending the numbers **1**, **2**, etc. Thus, for instance, **S1** and **S2** correspond to the singlet ground state of **1** and **2**, respectively. Tables 1 and 2 contain the relative energies of the different stationary points on each PES. A schematic energetic diagram of both PESs is also displayed in Figures 3 and 4.

The Cartesian coordinates of all structures reported, the total energies, and the harmonic vibrational frequencies calculated for the equilibrium structures are available as Supporting Information. Along with the vibrational frequencies, the IR intensity of each normal mode is also given.

**Table 1.** Dipole Moments ( $\mu$ , in Debye), ZPVE (kcal/mol), and Relative Energies (MRDCI+Q values in kcal/mol) for CASSCF-Optimized Structures of the Stationary Points on the Singlet PES

structure	$\mu$	ZPVE	MRDCI+Q <sup>a,b</sup>
<b>S1</b>	7.59	24.3	0.0 (0.0)
<b>S2</b>	3.67	24.1	-33.8 (-34.0)
<b>S3</b>	3.10	25.6	-148.8 (-147.5)
<b>STS1</b>	6.82	23.5	10.2 (9.4)
<b>STS2</b>	3.48	23.2	24.8 (23.7)
<b>STS3</b>	3.05	23.2	21.8 (20.7)
<b>STS4</b>	4.79	25.0	33.5 (34.2)
<b>STS5</b>	3.70	23.3	33.0 (32.0)

<sup>a</sup> The zero of energy is -264.92924 hartree. <sup>b</sup> The values in parentheses are ZPVE corrected.

**A. The Ground State PES. 1. Electronic Structure and Equilibrium Geometries of 1–3.** The most significant features of the optimized geometrical param-

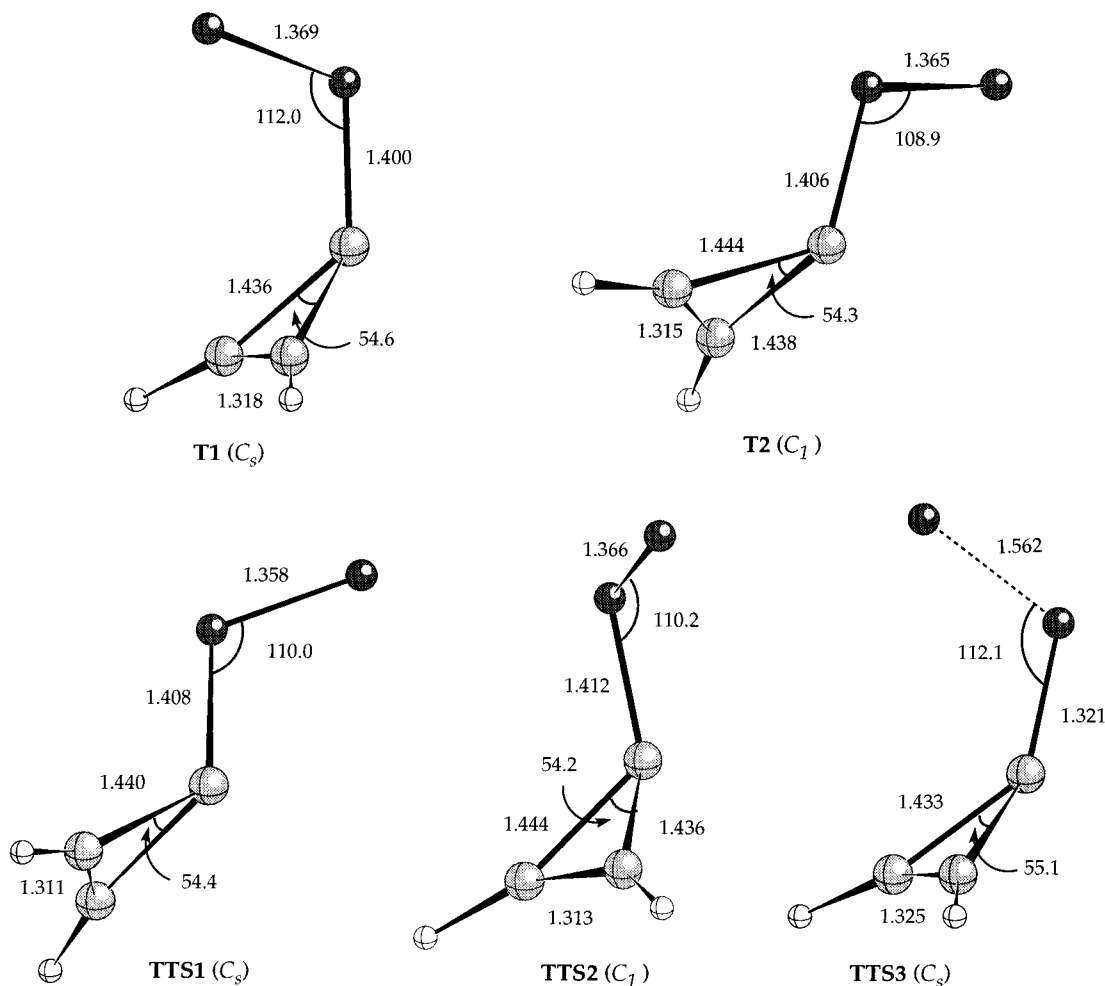


**Figure 2.** Selected geometrical parameters of the CASSCF-optimized structures for the stationary points located on the triplet potential energy surface. Distances are given in angstroms and angles in degrees.

**Table 2.** Dipole Moments ( $\mu$ , in Debye), ZPVE (kcal/mol), and Relative Energies (MRDCI+Q values in kcal/mol) for CASSCF-Optimized Structures of the Stationary Points on the Triplet PES

structure	$\mu$	ZPVE	MRDCI+Q <sup>a,b</sup>
<b>T1</b>	3.09	23.3	0.0 (0.0)
<b>T2</b>	3.35	23.3	5.6 (5.6)
<b>TTS1</b>	3.52	23.2	7.1 (7.0)
<b>TTS2</b>	3.17	23.2	6.2 (6.1)
<b>TTS3</b>	3.21	22.2	2.6 (1.5)

<sup>a</sup> The zero of energy is  $-264.89676$  hartree. <sup>b</sup> The values in parentheses are ZPVE corrected.

eters of **S1**, shown in Figure 1, are that the OO bond length is 1.559 Å while the CO bond length is 1.243 Å, suggesting single OO bond and double CO bond character, respectively. This result is in contrast to that found for the prototype  $\text{H}_2\text{CO}_2$  carbonyl oxide, which is calculated<sup>27</sup> to have OO and CO bond lengths of 1.366 and 1.283 Å, respectively, indicating a significant double bond character of both bonds. The remaining geometrical parameters of **S1** are in good agreement with the calculated for the ground state ( $^1A_1$ ) of cyclopropenyldiene.<sup>39,40</sup>

Both the CASSCF and MRDCI wave functions indicate that **S1** ( $C_s$  molecular symmetry) possesses a closed-shell

electronic structure, described mainly by the electronic configuration  $15a''^23a''^2$ . Therefore, the electronic state of **S1** is  $^1A_1$ . The three  $a''$  symmetry MOs are the  $\pi$  orbitals, corresponding to a lone pair on the terminal O atom, a  $\pi(\text{CO})$  bond, and a  $\pi(\text{CC})$  bond. Thus, **S1** has 6 $\pi$  electrons, and the  $\pi(\text{CO})$  and the  $\pi(\text{CC})$  bonds constitute a conjugate system. This electronic description suggests an important zwitterionic character of **S1**, as indicated by the large value (7.59 D) of the computed dipole moment; so **S1** corresponds to a  $[\text{cyclopropenone}]^+ [\text{O}]^-$  structure. This structure is also consistent with the atomic charges. Thus, the analysis of the Mulliken and Lowdin atomic populations show that the positive charge of **1** is totally located in the three-membered ring while the negative charge is mainly located at the terminal oxygen. The central oxygen has also a slightly negative charge. A significant zwitterionic character has also been found for the prototype  $\text{H}_2\text{CO}_2$  carbonyl oxide in recent high level ab-initio calculations.<sup>20i,27</sup>

The isomer **2** shows an equilibrium structure (**S2**) formed by two three-membered rings perpendicular to each other (see Figure 1). It possesses  $C_{2v}$  symmetry and is characterized by the electronic configuration  $9a_1^24b_1^2-4b_2^21a_2^2$ . The calculated OO (1.578 Å) and CO (1.387 Å) bond lengths, as well as the OCO bond angle ( $69.3^\circ$ ), are close to the experimental values of the unsubstituted dioxirane.<sup>41</sup> Comparing the remaining geometrical parameters with the corresponding of **S1**, it is clearly seen that the three-carbon atom ring does not suffer a significant change after cyclization of the COO part. The

(39) Bofill, J. M.; Farràs, J.; Olivella, S.; Solé, A.; Vilarrasa, J. J. *Am. Chem. Soc.* **1988**, *110*, 1694.

(40) CASSCF(4,4) geometry optimizations on  $X^1A_1$  of cyclopropenyldiene results in a CC bond distance of 1.417 Å and a CCC angle of  $55.3^\circ$ . The corresponding cartesian coordinates are provided as Supporting Information.

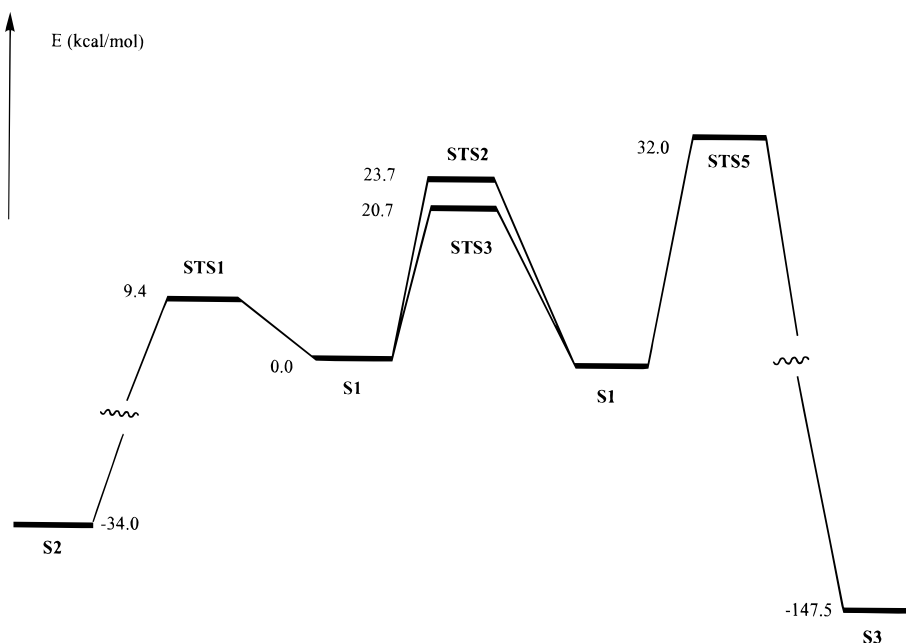


**Figure 3.** Schematic potential energy diagram showing the relative energies of the stationary points located on the singlet potential energy surface. The energy values were obtained from the ZPVE-corrected MRD-CI+Q energies relative to that of **S1**.

MRDCI calculations indicate that **S2** is 33.8 kcal/mol less energetic than **S1**. This value increases to 34.0 kcal/mol after inclusion of the ZPVE corrections.

The optimized geometrical parameters of formylketene **3** are shown in Figure 1, labeled as **S3**. It has  $C_s$  symmetry and is described by the electronic configuration  $15a'^2 3a''^2$ . The MRDCI calculations displayed in Table 1 indicate that **S3** is 148.8 kcal/mol (147.5 kcal/mol after ZPVE corrections) more stable than **1**. Consequently isomerization of **1** to **3** will be very exothermic.

**2. Isomerization of 1 to 2.** The isomerization of **1** to **2** involves mainly a movement of both O atoms without practically any change in the three-carbon-atom ring structure. The geometrical parameters of the transition structure (**STS1**) (see Figure 1), show that the CO and OO bond lengths (1.248 and 1.612 Å, respectively) have not changed very much with respect to the corresponding geometrical parameters of **1** (**S1**) (1.243 and 1.559 Å, respectively). The most important geometrical changes of **STS1** with respect to **S1** are a reduction of 21.7° in the COO angle and an increase of 59.6° of the dihedral angle between the COO and CCC planes. These geometrical parameters suggest that the saddle point **STS1** lies close to **1** on the reaction coordinate linking structures **1** and **2**. This feature is also supported by the dipole moment of 6.82 D calculated for **STS1**, which is closer to the value of 7.59 D calculated for **S1** than to the value of 3.67 D calculated for **S2**.

Table 1 and Figure 3 show that the computed energy barrier for the **1** → **2** cyclization is 10.2 kcal/mol (9.4 kcal/mol taking into account the ZPVE correction) at the MRDCI+Q level of theory. This value is about 14 kcal/mol lower than the calculated for the same process in the prototype  $H_2CO_2$ .<sup>27</sup> The lowest energy barrier required for the cyclization of **1** may be understood by looking at the differences in the geometrical parameters calculated for **S1** and  $H_2CO_2$ .<sup>27</sup> Thus, the geometrical parameters of  $H_2CO_2$  suggest an important amount of

double bond character of both CO and OO bonds, while the OO bond in **1** is essentially a single bond. Therefore the OO double bond in  $H_2CO_2$  should be broken in the cyclization process and this requires a greater amount of energy.

**3. Syn/Anti Isomerization.** Due to the  $C_s$  molecular symmetry conditions, the *syn* and *anti* isomers of **1** have the same structure. Previous theoretical studies<sup>17,20</sup> indicate two possible pathways for the *syn/anti* isomerization of the carbonyl oxides, namely through rotation about CO bond and via a linear COO structure. For the formal *syn/anti* isomerization of **1** we have considered both pathways.

**(a) CO Bond Rotation.** Rotation about the CO bond takes place through the breaking of the  $\pi(CO)$  bond. Consequently, an unpaired electron is mainly located on the corresponding  $C_3$  atom causing a pyramidalization of this atom. Therefore, depending on how the CO rotation is done, we have found two possible pathways for the *syn/anti* isomerization. The corresponding saddle points are labeled as **STS2** and **STS3**, respectively, in Figure 1. Both transition structures possess  $C_s$  symmetry and the same electronic structure ( $^1A'$ ). They also have nearly identical geometrical parameters except that in **STS2** the OO bond is directed in toward the three-carbon-atom ring and outwards in **STS3**. These results are similar to those found for the *syn/anti* isomerization of  $H_2CO_2$  and  $(CH_3)HCO_2$ .<sup>27</sup> As pointed out above, rotation about the CO bond involves a previous breaking of the double bond, and therefore a high energy barrier is expected for this process. The computed energy barrier (ZPVE corrected) is 20.7 kcal/mol for **STS3** and 23.7 kcal/mol for **STS2**. These transition structures lie more than 10 kcal/mol higher than the **STS1** one (see Table 1 and Figure 3). Therefore, it is expected that the *syn/anti* isomerization through CO bond rotation does not compete with the cyclization of **1** to **2**. It is also worth noting that the computed dipole moments of **STS2** (3.05 D) and **STS3** (3.48 D) are smaller than that of **S1** (7.59 D). Consequently, it seems reasonable to conclude that the *syn/anti* isomerization of **1** will not be favored in polar solvents.

(41) (a) Lovas, F. J.; Suenram, R. D. *Chem. Phys. Lett.* **1977**, *51*, 453. (b) Suenram, R. D.; Lovas, F. J. *J. Am. Chem. Soc.* **1978**, *100*, 5117.

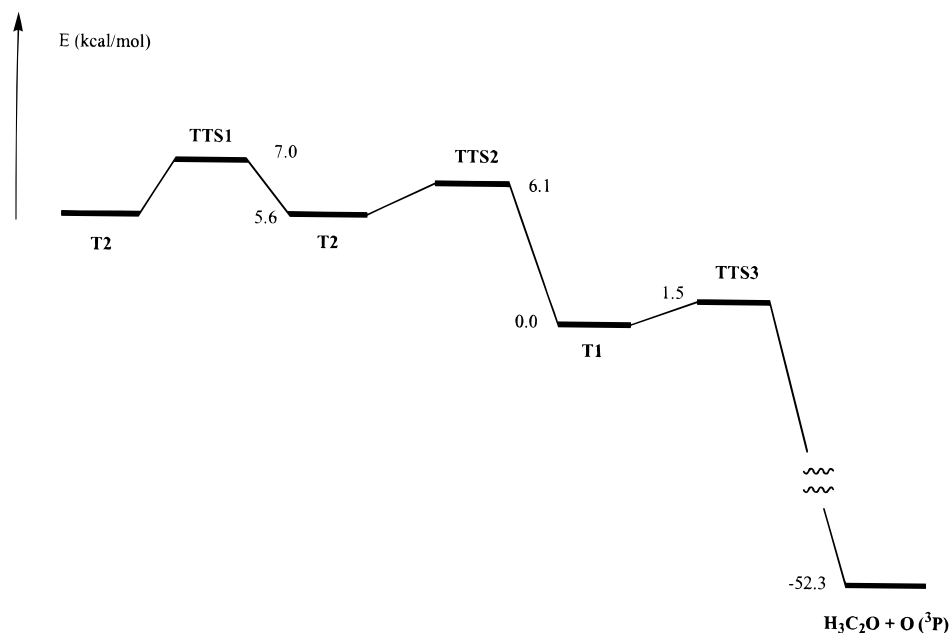


**Figure 4.** Schematic potential energy diagram showing the relative energies of the stationary points located on the triplet potential energy surface. The energy values were obtained from the ZPVE-corrected MRDCI+Q energies relative to that of **T1**. (a) The zero of energy is  $-264.92924$  hartree. (b) The values in parentheses are ZPVE corrected. (a) The zero of energy is  $-264.89676$  hartree. (b) The values in parentheses are ZPVE corrected.

**(b) Inversion at the Central Oxygen Atom.** The *syn/anti* isomerization via opening of the COO angle takes place through a linear COO structure of  $C_{2v}$  symmetry. This stationary point, labeled as **STS4**, is given in Figure 1. It is worth noting that the OO bond distance in **STS4** is  $0.559 \text{ \AA}$  longer than in **S1**. The analysis of the harmonic vibrational frequencies shows two imaginary frequencies ( $125.5i$  and  $61.2i \text{ cm}^{-1}$ ) and, therefore, **STS4** cannot be considered as a true transition state. The same feature was observed for  $\text{H}_2\text{CO}_2$  but with a much shorter OO bond length ( $1.493 \text{ \AA}$ ) in the structure of the corresponding stationary point.<sup>27</sup> Energetically, the MRDCI+Q calculation places **STS4**  $34.2 \text{ kcal/mol}$  above **S1** (see Table 1), a value that is more than  $10 \text{ kcal/mol}$  higher than the energies of **STS2** and **STS3**. Therefore we conclude that this pathway has no relationship to the *syn/anti* isomerization process.

**4. Isomerization of 1 to 3.** Isomerization of **1** to **3** involves a migration of the terminal oxygen to the carbon at position 4 in **1**. We have investigated if such a process would lead to the carbene **4** in a process similar to that described by Gutbrod et al.<sup>42</sup> for the OH abstraction in the prototype formaldehyde carbonyl oxide. However, a CASSCF investigation on carbene **4** indicates that any stationary point does not exist for this structure, and the optimization procedure leads to formylketene **3**. This result agrees with the calculations reported by Gutbrod et al. that found that the intermediate **5** in ref 42 is not a stationary point at the highest level of theory.

The lowest energy pathway we have found for the isomerization of **1** to **3** takes place in a single step via **STS5**. The most significant geometrical parameters of **STS5** (see Figure 1) are the CC and OO bond lengths ( $1.446$  and  $1.646 \text{ \AA}$ , respectively) and the COO angle ( $85.3^\circ$ ). Thus, the most important geometrical changes with respect to **S1** are an elongation of the CC double bond and of the OO bond of  $0.11$  and  $0.09 \text{ \AA}$ , respectively, and a reduction of  $21.2^\circ$  in the COO angle. Table 1 and

Figure 3 show that the energy barrier for the **1**  $\rightarrow$  **3** isomerization is  $33.0 \text{ kcal/mol}$  ( $32.0 \text{ kcal/mol}$  taking into account the ZPVE corrections) at the MRDCI+Q level of theory. This value is  $22.6 \text{ kcal/mol}$  higher than the energy barrier for the isomerization of **1** to **2**. Therefore, we conclude that formation of formylketene **3** will not compete with cyclization to cyclopropene dioxirane.

**B. The Lowest Triplet PES.** We have found five stationary points on the PES of the lowest triplet state. The corresponding optimized structures are displayed in Figure 2. Structures **T1** and **T2** are characterized as true local minima on the CASSCF PES, which correspond to the *endo* and *exo* conformations, respectively. Moreover, there exist two equivalent isomers of **T2**, which correspond to the change in the values of both dihedral angles in Figures 2. **TTS1** is a transition state connecting the two equivalent isomers of **T2**; **TTS2** is the transition structure connecting **T1** and **T2**, while **TTS3** is the transition structure linking **T1** with the dissociation products cyclopropenone ( $^1A_1$ ) and the O atom in its ground state ( $^3P$ ). Overall, the most remarkable geometrical features of all these stationary points are the strong pyramidalization at the  $C_3$  atom (see Figure 2) and the different degree of the rotation angle between the CCC and COO planes. Moreover, the geometrical structure of the CCC ring remains practically unchanged and close to that of the  $^3B_1$  state of cyclopropenylidene.<sup>43</sup>

Figure 4 shows that **T1** is predicted to be the lowest equilibrium structure on the triplet PES of **1**, and that the energy barriers of the different processes shown are very low (see also Table 2). Thus, the energy barrier for the dissociation of **T1** to ground state cyclopropenone ( $^1A_1$ ) plus the O atom ( $^3P$ ) is only of  $2.6 \text{ kcal/mol}$ . This value is reduced to  $1.5 \text{ kcal/mol}$  if the ZPVE corrections are taken into account. The corresponding transition structure (**TTS3**) resembles **T1** except in the OO and CO

(42) Gutbrod, R.; Schindler, R. N.; Kraka, E.; Cremer, D. *Chem. Phys. Lett.* **1996**, *252*, 221.

(43) CASSCF(4,4) geometry optimizations on  $^3B_1$  of cyclopropenylidene results in a CC bond distance of  $1.453 \text{ \AA}$  and a CCC angle of  $52.2^\circ$ . The corresponding cartesian coordinates are provided as Supporting Information.

bond distances, that are 0.193 and 0.079 Å longer and shorter, respectively. The triplet PES is placed energetically about 20.0 kcal/mol above the lowest energy point on the singlet PES, **S1**.

The analysis of the CASSCF and MRD-CI wavefunction indicates that the dominant electronic configuration of **T1** can be written as  $13a'^2 4a''^2 14a' 15a''$ , so it is of  $A''$  symmetry. The  $14a'$  MO is mainly located on  $C_3$  atom, while the  $5a''$  MO is mainly located on the terminal O atom, but with a significant OO bonding character. This feature is clearly reflected in the corresponding geometrical parameters. Thus, a comparison of the **S1** and **T1** structures (see Figures 1 and 2) reveals a lengthening of 0.157 Å in the CO distance and a shortening of 0.191 Å in the OO bond distance in going from the singlet to the triplet. As in the case of  $H_2CO_2$ ,<sup>27</sup> the CASSCF MOs indicate that the two unpaired electrons of the triplet state correspond to the electrons forming the  $\pi(CO)$  bond in the singlet ground state.

At this point it is worth noting that the geometries of **T1** and **STS3** are very similar to each other, and the same occurs for the geometries of **TTS1** and **STS2**. These results are easily rationalized by noting that in both cases the electronic wave function of these structures belongs to the same representation ( $A''$ ) of the molecular symmetry point group, so they are characterized by the same electronic configuration ( $\dots 14a' 15a''$ ). Consequently, it is expected that the energy differences between the singlet and triplet states of the same geometry should be very small, since this energy splitting is due mainly to the exchange integral between the two unpaired electrons. In fact, from the MRDCI+Q energies (Tables 2 and 3 of Supporting Information), **STS3** is calculated to lie only 1.4 kcal/mol above **T1** and **STS2** 2.7 kcal/mol below **TTS1**. The same situation was observed for  $H_2CO_2$  and  $(CH_3)HCO_2$ .<sup>27</sup> Therefore, it can be concluded that the energy barrier calculated for the *syn/anti* isomerization (via rotation about the CO bond) gives an estimation of the energetic position of the lowest triplet state.

**C. Dissociation of 1 into Cyclopropanone and Oxygen Atom.** The dissociation energy for the decomposition into cyclopropanone and atomic oxygen has been calculated for the lowest singlet and triplet states of **1**. Prior to the computation of the dissociation energy, a CASSCF geometry optimization was performed for the  $^1A_1$  ground state of cyclopropanone.<sup>44</sup> The corresponding Cartesian coordinates are available as Supporting Information.

The singlet ground state of **1** (**S1**) dissociates to yield cyclopropanone in its ground state and an oxygen atom in its  $^1D$  excited state. The process is endothermic with a computed dissociation energy of 19.3 kcal/mol (17.1 kcal/mol after the ZPVE correction).<sup>45</sup> Consequently, this dissociation will compete with the *syn/anti* isomerization, whose energy barrier is computed to be 20.7 kcal/mol (see Table 1). Here it is worth to note that the dissociation

energy of the parent  $H_2CO_2$  is computed to be 32.4 kcal/mol.<sup>27</sup> On the other hand, **T1** is predicted to dissociate into the ground state of cyclopropanone and the ground state of O atom ( $^3P$ ) through a highly exothermic process (51.1 kcal/mol or 52.3 kcal/mol after taking into account the ZPVE correction).<sup>45</sup> The corresponding energy barrier is very low as indicated in the previous section.

## Conclusions

From the theoretical study of the  $H_2C_3O_2$  PES presented above we emphasize the following points.

(1) The electronic structure of the singlet ground state of **1** can be viewed as a *zwitterion*. This is concluded from both the CASSCF-calculated equilibrium geometry and dipole moment.

(2) The COO ring in the cyclopropene dioxirane compound **2** shows an equilibrium structure very similar to that of the unsubstituted dioxirane. **2** is predicted to be about 34 kcal/mol more stable than the ground state of **1**. In the gas phase, the energy barrier for the isomerization of **1** to **2** is predicted to be about 9 kcal/mol.

(3) The energy barrier for the formal *syn/anti* isomerization process of the ground state of **1** is calculated to be about 21 kcal/mol. Therefore, it is expected that this process will not compete with the isomerization of **1** to **2**.

(4) Formylketene **3** is predicted to be about 148 kcal/mol more stable than **1**. However the gas phase energy barrier for the **1**  $\rightarrow$  **3** isomerization is evaluated to be 32 kcal/mol. Consequently this process will not compete with the isomerization of **1** to **2**.

(5) The dissociation of the singlet ground state **1** into the singlet ground state of the cyclopropanone ( $^1A_1$ ) and the lowest singlet state of oxygen atom ( $^1D$ ) is predicted to be endothermic by 17.1 kcal/mol. In contrast, the dissociation of the lowest triplet state into the triplet ground state of oxygen atom ( $^3P$ ) is predicted to be highly exothermic (52.3 kcal/mol) with an energy barrier of only 1.5 kcal/mol.

**Acknowledgment.** This research was supported by the Direcció General de Investigació Científica y Técnica (DGICYT Grants PB92-0796-C01 and PB92-0796-C02). The calculations described in this study were performed on the IBM RS6000 workstation and the SGI Power Challenge at the Centre d'Investigació i Desenvolupament del CSIC. We thank Professor Santiago Olivella (Universitat de Barcelona) for suggesting this study and for his valuable guidance. The authors also thank Professor Sigrid D. Peyerimhoff and Dr. Michael W. Schmidt for providing a copy of MRD-CI and GAMESS codes, respectively.

**Supporting Information Available:** Tables containing the Cartesian coordinates of all structures reported in this paper, the harmonic vibrational frequencies, and infrared intensities of the equilibrium structures (12 pages). This material is contained in libraries on microfiche, immediately follows this article in the microfilm version of the journal, and can be ordered from the ACS; see any current masthead page for ordering information.

JO962051D

(44) The optimized cartesian coordinates of cyclopropanone are provided as Supporting Information.

(45) The MRD-CI+Q energies of the dissociation products (hartrees) are:  $-74.89773$  ( $O(^3P)$ );  $-74.81809$  ( $O(^1D)$ ) and  $-190.08041$  (cyclopropanone ( $^1A_1$ )). The ZPVE of cyclopropanone is 22.1 kcal/mol.